Systems & Control Letters 178 (2023) 105584

Contents lists available at ScienceDirect

Systems & Control Letters

journal homepage: www.elsevier.com/locate/sysconle

Nonholonomic source seeking in three dimensions using pitch and yaw torque inputs[☆]

Raik Suttner[a,*], Miroslav Krstić[b]

[a] Institute of Mathematics, University of Wuerzburg, Wuerzburg, Germany
[b] Department of Mechanical and Aerospace Engineering, University of California, San Diego, USA

ARTICLE INFO

Article history:
Received 23 August 2022
Received in revised form 12 May 2023
Accepted 12 June 2023
Available online 30 June 2023

Keywords:
Source seeking
Nonholonomic systems
Averaging
Symmetric product approximations
Practical stability

ABSTRACT

We study the problem of source seeking without position measurements in three-dimensional Euclidean space. The source-seeking agent is modeled by a second-order dynamical system with nonholonomic velocity constraints. A constant thrust leads to a uniform forward motion, while the agent's orientation can be influenced through two torque inputs. Our control law extends a recently introduced source seeking method for a torque-controlled unicycle. The proposed feedback law involves perturbation signals with sufficiently large amplitudes and frequencies. The closed-loop system can be written as an affine connection system, which approximates the behavior of an averaged system. This averaged system is driven into the direction of symmetric products of vector fields from the closed-loop system. Our feedback law is designed in such a way that the symmetric products contain gradient information about the unknown signal function. Under suitable assumptions on the signal function, we prove practical local uniform asymptotic stability for the closed-loop system.

1. Introduction

The problem of source seeking without position measurements occurs when an autonomous agent aims to locate an extreme point of a scalar signal in an environment that denies access to a global positioning system. For instance, in case of an underwater vehicle, position measurements and communications with the outside world are difficult to realize, especially in dark conditions, and in surveillance/reconnaissance tasks where active acoustic sensing is not allowed. Also vehicles under ice or in caves may be unable to determine their current position. In such an environment, locating the unknown source of a signal becomes a challenging problem. The signal could be given by the pressure of acoustic waves or by the strength of an electromagnetic field. It is assumed that the agent is equipped with a suitable sensor so that it can measure the value of the signal at the current (unknown) position. Clearly, a suitable source seeking strategy must be adapted to the agent's equations of motion and to how the agent is actuated.

Many of the existing studies on source seeking propose algorithms for agents in the two-dimensional plane [1–3]. A frequently considered agent model is that of a kinematic unicycle as, for example, in [4–7]. So far, only a few papers address the problem of source seeking in three dimensions. Of particular interest are methods for three-dimensional vehicle models with nonholonomic velocity constraints and a uniform forward motion. This is motivated by potential applications to aerial and underwater vehicles. To the best of our knowledge, all of the existing studies on three-dimensional source seeking with underactuated vehicles consider velocity-controlled kinematic models. (In the present paper, we propose a method for a second-order dynamic agent model.) An example of a three-dimensional kinematic model is a **v**ehicle **y**aw-like and **p**itch **a**ctuated (VYPa). An implementation of this model requires measurements of the pitch angle to realize the yaw-like velocity. Perturbation-based source seeking methods for the kinematic VYPa model are proposed in [8–10]. A hybrid controller for a similar kinematic model is presented [11]. The method in [12] for the kinematic VYPa model extracts gradient information from computations of Poisson integrals under the assumption that the sensed signal is given by a harmonic function. A perturbation-based method for a roll and yaw velocity-actuated kinematic model with constant forward velocity is proposed in [13]. Methods for three-dimensional underactuated kinematic models with oscillatory translational velocity are presented in [14,15].

In the present paper, we propose a source seeking strategy for a dynamic version of the above-mentioned kinematic VYPa model. The control inputs of the dynamic VYPa model are two torques. Such a torque-actuated model is expected to provide a

☆ This research was supported by the German Research Foundation DFG, project number DA 767/13-1.
* Corresponding author.
E-mail addresses: raik.suttner@mathematik.uni-wuerzburg.de (R. Suttner), krstic@ucsd.edu (M. Krstić).

https://doi.org/10.1016/j.sysconle.2023.105584
0167-6911/

more realistic description of a mechanical system than a velocity-actuated model. The velocity of a first-order kinematic system can be changed instantaneously through the inputs to any prescribed value. However, this is not possible for a second-order dynamic system because of the system's inertia. For this reason, controlling the dynamic VYPa model is also more challenging than controlling the kinematic VYPa model.

In our previous work [16], we have proposed a source seeking method for a torque-controlled unicycle with uniform forward velocity. The VYPa model reduces to the unicycle model if the pitch angle is equal to zero. It is therefore reasonable to expect that the approach in [16] might serve as a basis for a source seeking method for the dynamic VYPa model. Indeed, we will see that the control law from [16] is also useful for the yaw-like torque input of the dynamic VYPa model. This yaw-like torque stabilizes the vehicle about the source within a certain plane. The additional input for the pitch moment stabilizes the vehicle about the source vertically to the plane. These statements will be proved by means of a suitable averaging and stability analysis in the main part of the paper.

To construct a source seeking method for the dynamic VYPA model, we follow a recently established approach to design extremum seeking control for mechanical systems. This approach is based on the averaging results in [17] for mechanical systems under vibrational control. It is known from [17] that certain large-amplitude high-frequency perturbation signals provide access to so-called *symmetric products* of vector fields, which originate from iterated Lie brackets of vector fields on the tangent bundle of the configuration manifolds. A suitably designed feedback law can lead to the effect that the symmetric products provide information about the gradient of the unknown objective function. Several extremum seeking problems have been already solved by control laws based on symmetric product approximations. This includes source seeking control for unicycles [16,18,19] and two-dimensional water vessels [20], formation shape control for double-integrator point masses [21], and extremum seeking control for certain classes of fully-actuated mechanical systems without velocity constraints [22,23]. However, none of the above methods can be successfully applied to the nonholonomic three-dimensional vehicle that we study in this paper. The complex dynamics of the vehicle demand a different control strategy. In the present paper, we show how such a control law can be designed using approximations of symmetric product. Our control law involves only one oscillatory perturbation signal for each input channel, which indicates the conceptual difference from extremum seeking methods based on approximations of Lie brackets of pairs of vector fields as in [24–26] with two phase-shifted oscillatory signals for each input channel. In contrast to extremum seeking control for open-loop stable systems as in [27–29] (which is justified in certain applications, see e.g. [30–32]), our method employs sufficiently strong perturbation signals to overpower potentially unstable dynamics.

The proposed source seeking method employs oscillatory torque inputs with sufficiently large amplitudes and frequencies. Such inputs are certainly difficult (and sometimes even impossible) to realize in practical implementations. In the present paper, we do not address the difficult problem of implementations in real-world vehicles, which is, of course, relevant to practitioners. Instead, we focus on the underlying theoretical principles that allow us to design the first source seeking method for the dynamic VYPa model.

The paper is structured as follows. The subsequent Section 2 introduces a suitable notion of practical stability for the closed-loop system. A detailed description of the dynamic VYPa model can be found in Section 3. The source seeking problem and its solution are presented in Section 4. An averaging analysis in Section 5 will reveal that the proposed control leads to an approximations of symmetric products as indicated earlier. The symmetric products involve the gradient of the signal function and stabilize the system, which is proved in Section 6. Finally, in Section 7, we provide numerical simulations to illustrate our stability result.

2. Practical stability

Let $|\cdot|$ denote the Euclidean norm on $\mathbb{R}^n$ and let U be an open subset of $\mathbb{R}^n$. For every positive real number ω, let f^ω be a time-dependent vector field on U. We assume that, for every $\omega > 0$, every $t_0 \in \mathbb{R}$, and every $x_0 \in U$, the ordinary differential equation

$$\dot{x} = f^\omega(t, x) \tag{1}$$

with initial condition $x(t_0) = x_0$ has a unique maximal solution, which may have a finite escape time. Our control law will result in a closed-loop system of the form (1), where ω is a parameter to scale the amplitudes and frequencies of the employed perturbation signals. To reveal the behavior of the closed-loop system for large values of ω, we will apply a suitable change of variables. More generally, for every $\omega > 0$ and every $t \in \mathbb{R}$, we suppose that $\phi_t^\omega : U \to U$ is a bijective map and we consider the change of variables

$$\tilde{x} = \phi_t^\omega(x). \tag{2}$$

We will use the following notion of stability to describe the behavior of the closed-loop system.

Definition 1 (*[33]*)**.** A point x_* of U is said to be *practically locally uniformly asymptotically stable* for (1) in the variables (2) if the following conditions are both satisfied.

1. *Practical uniform stability*: For every $\varepsilon > 0$, there exist $\delta, \omega_0 > 0$ such that, for every $\omega \geq \omega_0$, every $t_0 \in \mathbb{R}$, and every $\tilde{x}_0 \in U$ with $|\tilde{x}_0 - x_*| \leq \delta$, the maximal solution x of (1) with initial condition $x(t_0) = (\phi_t^\omega)^{-1}(\tilde{x}_0)$ satisfies $|\phi_t^\omega(x(t)) - x_*| \leq \varepsilon$ for every $t \geq t_0$.
2. *Practical local uniform attraction*: There exists $\delta > 0$ such that, for every $\varepsilon > 0$, there exist $\tau, \omega_0 > 0$ such that, for every $\omega \geq \omega_0$, every $t_0 \in \mathbb{R}$, and every $\tilde{x}_0 \in U$ with $|\tilde{x}_0 - x_*| \leq \delta$, the maximal solution x of (1) with initial condition $x(t_0) = (\phi_t^\omega)^{-1}(\tilde{x}_0)$ satisfies $|\phi_t^\omega(x(t)) - x_*| \leq \varepsilon$ for every $t \geq t_0 + \tau$.

Remark 1. In Definition 1, the word "practically" emphasizes the dependence on the parameter ω and the word "uniformly" means uniformity with respect to the time parameter. If there exists a vector field f on U such that $f^\omega(t, x) = f(x)$ and if $\phi_t^\omega(x) = x$ for every $\omega > 0$, every $t \in \mathbb{R}$, and every $x \in U$, then we omit the words "practically" and "uniformly". In this case, Definition 1 reduces to the usual notion of local asymptotic stability.

Let $\bar{f}$ be a vector field on U. We assume that, for every $\bar{x}_0 \in U$, the ordinary differential equation

$$\dot{\bar{x}} = \bar{f}(\bar{x}) \tag{3}$$

with initial condition $\bar{x}(0) = \bar{x}_0$ has a unique maximal solution. We will see in Section 5 that the oscillatory closed-loop system of the form (1) approximates the behavior of an averaged system of the form (3) in the following sense.

Definition 2 (*[33]*)**.** We say that solutions of (1) in the variables (2) *approximate the solutions* of (3) if, for all $\varepsilon, \Delta > 0$ and every compact subset K of U, there exists $\omega_0 > 0$, such that, for every

$t_0 \in \mathbb{R}$ and every $\bar{x}_0 \in U$, the following implication holds: If the maximal solution $\bar{x}$ of (3) with initial condition $\bar{x}(t_0) = \bar{x}_0$ satisfies $\bar{x}(t) \in K$ for every $t \in [t_0, t_0 + \Delta]$, then, for every $\omega \geq \omega_0$, the maximal solution x of (1) with initial condition $x(t_0) = (\phi_t^\omega)^{-1}(\bar{x}_0)$ satisfies $|\phi_t^\omega(x(t)) - \bar{x}(t)| \leq \varepsilon$ for every $t \in [t_0, t_0 + \Delta]$.

If the solutions of (1) in the variables (2) approximate the solutions of (3), then certain stability properties of (3) carry over to (1). This statement is made precise by the following result.

Proposition 1 ([33]). *Assume that the solutions of (1) in the variables (2) approximate the solutions of (3). Then, for every point x_* of U, the following implication holds: If x_* is locally asymptotically stable for (3), then x_* is practically locally uniformly asymptotically stable for (1) in the variables (2).*

3. Description of the VYPa model

In this section, we first recall the kinematic model of a **v**ehicle **y**aw-like and **p**itch **a**ctuated (VYPa) from [8] (and also [9,10,12,14]), and then we extend it to a dynamic model. The model is sketched in Fig. 1. Let e_1, e_2, e_3 be the standard unit vectors of $\mathbb{R}^3$ and let $\langle \cdot, \cdot \rangle$ denote the Euclidean inner product on $\mathbb{R}^3$. The vectors e_1, e_2, e_3 define the axes of a fixed reference frame. The current orientation of the vehicle is described by a rotation matrix $R \in \mathrm{SO}(3)$ and the orthonormal vectors Re_1, Re_2, Re_3 define the axes of the body frame. It is assumed that the orientation of the vehicle is restricted to the subset

$$O \;:=\; \big\{ R \in \mathrm{SO}(3) \;\big|\; \langle e_3, Re_2 \rangle = 0,\; \langle e_3, Re_3 \rangle > 0 \big\} \tag{4}$$

of SO(3). Note that O is not a subgroup of SO(3) and that O is not commutative (i.e., there exist $R_1, R_2 \in O$ such that $R_1R_2 \neq R_2R_1$). The restriction of the orientation to elements of O excludes roll motions about Re_1. Let $\times$ denote the usual cross product on $\mathbb{R}^3$. For every $R \in O$, we have

$$e_3 \times Re_3 \;=\; \sin(\alpha(R))(-Re_2), \tag{5}$$

where

$$\alpha \;=\; \alpha(R) \;:=\; \arcsin(\langle e_3 \times Re_3, -Re_2 \rangle) \tag{6}$$

is the *pitch angle* between the e_3-reference axis and the Re_3-body axis. Note that $\alpha(R) \in (-\pi/2, \pi/2)$ for every $R \in O$. We frequently suppress the dependence of α on $R \in O$ in the notation. It is assumed that the vehicle can measure α at any time. It is further assumed that the orientation of the vehicle can be controlled through two types of on-board actuators. The first type of actuators generates a pitch moment about $-Re_2$. The second type of actuators is assumed to generate a yaw-like moment about e_3. Because of the measurements of α for every $R \in O$, such a yaw-like moment can be realized by movable actuators that generate a torque about the axis that originates from a rotation of Re_3 about Re_2 by the angle α. Suitably aligned actuators for this purpose are shown in Fig. 1. Alternatively, for each $R \in O$, a torque about the e_3-reference axis can also be realized by the α-dependent superposition

$$\sin(\alpha)\,Re_1 + \cos(\alpha)\,Re_3 \;=\; e_3 \tag{7}$$

of torques about the Re_1- and Re_3-body axes. Infinitesimal rotations of the vehicle about $-Re_2$ and e_3 are compatible with the set O of admissible orientations. Using the rank theorem, one can prove in fact the following statement.

Remark 2. The set O is a two-dimensional embedded submanifold of SO(3) and, for every $R \in O$, the tangent space T_RO to O at R is given by

$$T_RO \;=\; \mathrm{span}\{-R\widehat{e_2},\; \sin(\alpha(R))\,R\widehat{e_1} + \cos(\alpha(R))\,R\widehat{e_3}\}, \tag{8}$$

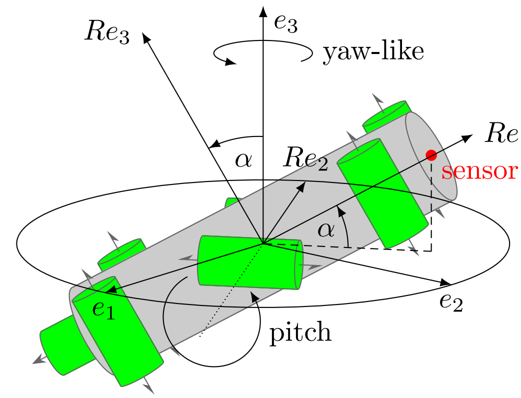

Fig. 1. Illustration of the VYPa model. The vehicle has body-fixed actuators to generate a pitch moment about $-Re_2$ and movable actuators to generate a yaw-like moment about e_3. Another body-fixed actuator induces a forward motion into the direction of Re_1.

where the vector space isomorphism $\widehat{\cdot} : \mathbb{R}^3 \to \mathfrak{so}(3)$ is defined by

$$\widehat{\Omega} \;:=\; \begin{bmatrix} 0 & -\Omega^3 & \Omega^2 \\ \Omega^3 & 0 & -\Omega^1 \\ -\Omega^2 & \Omega^1 & 0 \end{bmatrix}, \tag{9}$$

and $\mathfrak{so}(3)$ denotes the tangent space to SO(3) at the identity.

Because of Remark 2, well-defined smooth **p**itch and **y**aw-like vector fields X_p and X_y on O are given by

$$X_\mathrm{p}(R) \;:=\; -R\widehat{e_2}, \tag{10}$$

$$X_\mathrm{y}(R) \;:=\; \sin(\alpha(R))\,R\widehat{e_1} + \cos(\alpha(R))\,R\widehat{e_3} \tag{11}$$

with $\alpha(R)$ as in (6). The manifold O and the vector fields X_p, X_y also appear in [8–10,12,14], but they are represented by a parametrization as follows.

Remark 3. Define $\Phi : \mathbb{R}^3 \to \mathrm{SO}(3)$ by

$$\Phi(\phi, \alpha, \theta) \;:=\; \exp(\theta\widehat{e_3})\exp(-\alpha\widehat{e_2})\exp(\phi\widehat{e_1}), \tag{12}$$

where $\exp : \mathfrak{so}(3) \to \mathrm{SO}(3)$ is the matrix exponential function and $\widehat{\cdot} : \mathbb{R}^3 \to \mathfrak{so}(3)$ is defined by (9). Then, we have $\Phi(0, \alpha, \theta) \in O$ and

$$X_\mathrm{p}(\Phi(0, \alpha, \theta)) \;=\; \frac{\partial \Phi}{\partial \alpha}(0, \alpha, \theta), \tag{13}$$

$$X_\mathrm{y}(\Phi(0, \alpha, \theta)) \;=\; \frac{\partial \Phi}{\partial \theta}(0, \alpha, \theta) \tag{14}$$

for every $\alpha \in (-\pi/2, \pi/2)$ and every $\theta \in \mathbb{R}$. The second argument of Φ is the same as the pitch angle α in (6).

The configuration manifold Q of the VYPa model is the set $\mathbb{R}^3 \times O$ with the submanifold O of SO(3) as in (4). An element $(p, R) \in Q$ represents the position $p \in \mathbb{R}^3$ of the vehicle center and the orientation $R \in O$ of the vehicle. It is assumed that the translational motion of the vehicle is restricted by nonholonomic velocity constraints such that

$$\dot{p} \;=\; v\,Re_1, \tag{15a}$$

where $v \in \mathbb{R}$ is the translational velocity component. The vehicle is moving forward if v is positive. A uniform forward motion is preferred. Fig. 1 shows a suitably placed actuator along the Re_1-body axis for this purpose. Since $X_\mathrm{p}(R)$ and $X_\mathrm{y}(R)$ span the tangent space to O at every $R \in O$, we can write the rotational velocity as

$$\dot{R} \;=\; \Omega^\mathrm{p}\,X_\mathrm{p}(R) + \Omega^\mathrm{y}\,X_\mathrm{y}(R), \tag{15b}$$

where Ω^{p} and Ω^{y} are the **p**itch velocity and the **y**aw-like velocity, respectively. For the kinematic VYPa model in [8–10,12], the translational velocity component v is a positive constant and the velocities Ω^{p}, Ω^{y} serve as inputs. Here, we consider a dynamic (second-order) VYPa model in which v, Ω^{p}, Ω^{y} are given by the differential equations

$$m\,\dot{v} \;=\; a - k\,v, \tag{15c}$$

$$J_{\mathrm{p}}\,\dot{\Omega}^{\mathrm{p}} \;=\; \tau^{\mathrm{p}} - \kappa_{\mathrm{p}}\,\Omega^{\mathrm{p}}, \tag{15d}$$

$$J_{\mathrm{y}}\,\dot{\Omega}^{\mathrm{y}} \;=\; \tau^{\mathrm{y}} - \kappa_{\mathrm{y}}\,\Omega^{\mathrm{y}}, \tag{15e}$$

where τ^{p}, τ^{y} are torque inputs and a, m, J_{p}, J_{y}, k, κ_{p}, κ_{y} are unknown positive real constants. One may interpret m as the body mass and $J_{\mathrm{p}}, J_{\mathrm{y}}$ can be seen as moments of inertia. The terms $-k\,v$, $-\kappa_{\mathrm{p}}\,\Omega^{\mathrm{p}}$, and $-\kappa_{\mathrm{y}}\,\Omega^{\mathrm{y}}$ model the impact of linear damping; for example, due to air resistance. In (15c), the constant $a > 0$ describes a constant forward force, which leads to convergence of the translational velocity v to the forward velocity a/k. In summary, the dynamic VYPa model is the nonholonomic second-order system (15) with configuration manifold $Q = \mathbb{R}^3 \times O$ and two inputs τ^{p} and τ^{y} to control the pitch and yaw-like moment about $-Re_2$ and e_3, respectively.

Remark 4. The nonholonomic velocity constraints for the translational motion in (15a) only allow changes of the position along the direction of the alignment vector Re_1. In reality, however, one can expect that a vehicle (such as an aerial vehicle) will also have a lateral velocity along the direction of Re_2 due to Coriolis effects and a vertical velocity along the direction of Re_3 due to gravity. The VYPa model does not take these (undesired) velocities into account. Therefore, in some sense, one may say that the nonholonomic velocity constraints simplify the problem of source seeking since the constraints prevent undesired drifts into the lateral and vertical direction. It is considerably more challenging to design a source seeking method for an underacted torque-controlled vehicle without nonholonomic velocity constraints.

4. Problem statement and control law

Next we formulate the control problem for the dynamic VYPa model (15) and propose a solution. As explained in the previous section, we assume that the vehicle can measure the pitch angle α in order to generate a yaw-like moment about the e_3-axis. The remaining state variables are not assumed to be measurable by the vehicle. In particular, the vehicle cannot determine its current position with respect to a references frame. Also the velocity components v, Ω^{p}, and Ω^{y} in (15c)–(15e) are unknown quantities. The only additional information about the current system state is given by real-time measurements of a purely position-dependent scalar signal. To this end, the vehicle is equipped with a suitable sensor so that it can measure the signal value at any time. We assume that the signal is given by a smooth real-valued function ψ on $\mathbb{R}^3$, which is subsequently referred to as the *signal function*. However, we do not assume that the signal function ψ is analytically known. The vehicle can only measure the value of ψ at the current position of the sensor. Moreover, the vehicle cannot store data to compare different measurement results at different time instances.

We consider the signal function ψ as a cost (or objective) function. We are interested in a control law for the dynamic VYPa model (15) that asymptotically stabilizes the vehicles about positions where ψ attains a minimum value. A minimum point of ψ is called a *source* of the signal. Here, we propose a perturbation-based approach to seek a source. That is, we feed in suitable oscillatory perturbation signals and extract information about the gradient of ψ from the response of the measured value of ψ at the position of the sensor. Note that the inputs τ^{p} and τ^{y} in (15) have a direct impact on the vehicle's orientation, but the value of ψ only depends on the position. Therefore, it is reasonable to attach the sensor to the vehicle in such a way that changes in the vehicle's orientation lead to changes in the sensor's position. We follow the approach in [8] (and also [9,10,14]) and place the sensor at the point $p + \rho\,Re_1$, where $\rho > 0$ is the fixed (but unknown) distance of the sensor to the position $p \in \mathbb{R}^3$ of the vehicle center. Such a displaced sensor is also indicated in Fig. 1. A measurement of ψ in the current configuration $(p, R) \in Q$ results in the real number

$$y \;=\; \psi(p + \rho\,Re_1). \tag{16}$$

One may view (16) as the *output* of the VYPa model (15).

Now we introduce the constituents of the proposed source seeking method. Let T be a positive real number. Our control law employs perturbation signals, which are generated by measurable, bounded, T-periodic functions $u^{\mathrm{p}}, u^{\mathrm{y}} : \mathbb{R} \to \mathbb{R}$ with zero mean. To avoid undesired interferences between u^{p}, u^{y}, we demand that their zero-mean anti-derivatives $U^{\mathrm{p}}, U^{\mathrm{y}} : \mathbb{R} \to \mathbb{R}$ satisfy the orthonormality condition

$$\frac{2}{T}\int_0^T U^i(\sigma)\,U^j(\sigma)\,\mathrm{d}\sigma \;=\; \begin{cases} 1 & \text{if } i = j, \\ 0 & \text{if } i \neq j \end{cases} \tag{17}$$

for all $i, j \in \{\mathrm{p}, \mathrm{y}\}$. For instance, if $T = 2\pi$, then we can define u^{p} and u^{y} by $u^{\mathrm{p}}(\sigma) := \cos(\sigma)$ and $u^{\mathrm{y}}(\sigma) := 2\cos(2\sigma)$, respectively. To incorporate measurements of the output (16) in a suitable way into our feedback law, we introduce two *design functions* $\beta, \gamma_h : \mathbb{R} \to \mathbb{R}$, where the second function, γ_h, depends on a parameter $h > 0$. For the moment, we only demand that β and γ_h are smooth. Later, in Section 6, we will narrow the class of suitable design functions by requiring additional properties of β and γ_h. Finally, let λ be a positive real constant. We propose the feedback law

$$\tau^{\mathrm{p}} \;=\; -\lambda\,\sin\alpha + \omega\,u^{\mathrm{p}}(\omega t)\,\beta(y - \eta), \tag{18a}$$

$$\tau^{\mathrm{y}} \;=\; \omega\,u^{\mathrm{y}}(\omega t)\,\gamma_h(h\,(y - \eta)) \tag{18b}$$

for the dynamic VYPa model (15), where h and ω are (sufficiently large) positive real control parameters, α is the measured pitch angle in (6), y is the measured signal value in (16), and η is the real-valued state of the filter

$$\dot{\eta} \;=\; h\,(y - \eta) \tag{19}$$

with filter input y and filter output $y - \eta$. We note that an implementation of the proposed feedback law (18) requires neither position measurements nor knowledge of the gradient of the unknown signal function.

The closed-loop system is obtained by substituting (18) into (15). An averaging analysis in Section 5 will reveal that the closed-loop system approximates the behavior of a certain averaged system if the control parameter $\omega > 0$ is sufficiently large. We will also see in Section 5 that the averaged system can be written as system (15) under the control law

$$\tau^{\mathrm{p}} \;=\; -\lambda\,\sin\alpha - \tfrac{1}{2}\,\tfrac{\rho}{J_{\mathrm{p}}}\,(\beta\beta')(y - \eta) \tag{20a}$$

$$\cdot\,\langle \operatorname{grad}\psi(p + \rho\,Re_1), Re_3\rangle, \tag{20b}$$

$$\tau^{\mathrm{y}} \;=\; -\tfrac{1}{2}\,\tfrac{\rho}{J_{\mathrm{y}}}\,h\,(\gamma_h\gamma_h')(h\,(y - \eta))\,\cos\alpha \tag{20c}$$

$$\cdot\,\langle \operatorname{grad}\psi(p + \rho\,Re_1), Re_2\rangle, \tag{20d}$$

where $(\beta\beta')(x)$ denotes the product of β and its derivative β' evaluated at some $x \in \mathbb{R}$, and $(\gamma_h\gamma_h')(x)$ is defined correspondingly. Note that the inner products in (20b) and (20d) involve the unknown gradient of ψ. We will choose the design functions β and γ_h in such a way that the products $\beta\beta'$ and $\gamma_h\gamma_h'$ in (20a) and (20c) always attain positive values. Then, we have access to the negative directional derivatives of ψ along Re_3 and Re_2. Moreover, if the pitch angle α is close to 0, then the directional derivative of ψ along Re_3 in (20b) is approximately the same as the directional derivative of ψ along e_3. This indicates that the second term on the right-hand side of (20a), (20b) minimizes ψ with respect to its third argument (i.e., along the e_3-axis). The first term on the right-hand side of (20a), (20b) asymptotically stabilizes the pitch angle α about 0. Next, we indicate the impact of (20c), (20d) on the VYPa model (15). Recall that the constant force in (15c) leads to a non-zero constant forward velocity. For this reason, we cannot expect that the position of the vehicle converges to a minimum point of ψ. However, if we induce a suitable yaw-like moment, then we can at least ensure that the vehicle tends to a motion around a minimum point. This is done by means of the directional derivative of ψ along Re_2 in (20d). If the directional derivative of ψ along Re_2 is negative, then a minimum point is to the left of the vehicle and the torque in (20c), (20d) causes a counter-clockwise motion. Conversely, if the directional derivative of ψ along Re_2 is positive, then a minimum point is to the right of the vehicle and the torque in (20c), (20d) causes a clockwise motion. Thus, in summary, we can expect that, under suitable assumptions, the inputs in (20) lead to a vanishing pitch angle, minimization of ψ with respect to third argument, and a motion of the vehicle around a minimum point of ψ. If $\omega > 0$ is sufficiently large, then approximately the same effect occurs for the inputs in (18).

Finally, we indicate the intention of the design function γ_h and its dependence on the parameter h. One can show that, in general, a constant multiple of the gradient term in (20d) does not lead to an asymptotically stable motion of the vehicle around a minimum point of ψ. However, asymptotic stability can be induced if the gradient term in (20d) is amplified and reduced in a suitable way. This is done by means of the scaling factor $h(\gamma_h\gamma_h')(h(y-\eta))$ in (20c). Note that, if the parameter $h > 0$ is sufficiently large, then $h(y-\eta)$ approximates the time derivative of the sensed signal y. We will choose the design function γ_h in such a way that the product $\gamma_h\gamma_h'$ is a strictly increasing function. Then, depending on whether y is increasing or decreasing, the scaling factor $h(\gamma_h\gamma_h')(h(y-\eta))$ amplifies or reduces the yaw-like moment in (20c), (20d). Such a scaling can lead to the desired effect that the vehicle converges to certain levels set of the signal function. To derive a simple stability result, we will also demand that the equilibrium value $h(\gamma_h\gamma_h')(0)$ of the scaling factor is independent of h. All required properties of the design functions β and γ_h that we need to prove stability are made precise later in Assumptions 3 and 5.

By applying the feedback law (18), (19) to the dynamic VYPa model (15), we obtain the closed-loop system

$$\dot p = v\,Re_1, \tag{21a}$$
$$\dot R = \Omega^{\mathrm p} X_{\mathrm p}(R) + \Omega^{\mathrm y} X_{\mathrm y}(R), \tag{21b}$$
$$m\,\dot v = a - k\,v, \tag{21c}$$
$$J_{\mathrm p}\,\dot\Omega^{\mathrm p} = -\kappa_{\mathrm p}\,\Omega^{\mathrm p} - \lambda\,\sin(\alpha(R)) + \omega\,u^{\mathrm p}(\omega t)\,\beta\big(\xi(p,R,\eta)\big), \tag{21d}$$
$$J_{\mathrm y}\,\dot\Omega^{\mathrm y} = -\kappa_{\mathrm y}\,\Omega^{\mathrm y} + \omega\,u^{\mathrm y}(\omega t)\,\gamma_h\big(h\,\xi(p,R,\eta)\big), \tag{21e}$$
$$\dot\eta = h\,\xi(p,R,\eta), \tag{21f}$$

where the real-valued function ξ on $\mathbb{R}^3 \times O \times \mathbb{R}$, defined by

$$\xi(p,R,\eta) := \psi(p+\rho\,Re_1) - \eta, \tag{22}$$

describes the difference $y-\eta$ in (18) and (19).

5. Averaging analysis

Now we explain in more detail why the inputs in (18) have approximately the same effect on (15) as the inputs in (20) if the parameter $\omega > 0$ is sufficiently large. To this end, we write the closed-loop system (21) as a so-called affine connection system on the configuration manifold $Q = \mathbb{R}^3 \times O$. The reader is referred to the textbook [34] for an introduction to affine connection systems and approximations of symmetric product.

Since the configuration manifold Q is the Cartesian product of $\mathbb{R}^3$ and O, for every point $q = (p,R)$ of Q, the tangent space to Q at q can be written as the Cartesian product of $\mathbb{R}^3$ and the tangent space to O at R. Recall that the tangent space to O at R is spanned by the vectors $X_{\mathrm p}(R)$ and $X_{\mathrm y}(R)$ in (10) and (11). Thus, we can define vector fields $Z_{\mathrm t}$, $Z_{\mathrm p}$, $Z_{\mathrm y}$, Y_0, $Y_{\mathrm p}$, $Y_{\mathrm y}$ on Q by

$$Z_{\mathrm t}(q) := (Re_1, 0), \tag{23}$$
$$Z_{\mathrm p}(q) := (0, X_{\mathrm p}(R)), \tag{24}$$
$$Z_{\mathrm y}(q) := (0, X_{\mathrm y}(R)), \tag{25}$$
$$Y_0(q) := \tfrac{a}{m}\,Z_{\mathrm t}(q) - \tfrac{\lambda}{J_{\mathrm p}}\,\sin(\alpha(R))\,Z_{\mathrm p}(q), \tag{26}$$
$$Y_{\mathrm p}(q) := \tfrac{1}{J_{\mathrm p}}\,\beta\big(\xi(p,R,\eta)\big)\,Z_{\mathrm p}(q), \tag{27}$$
$$Y_{\mathrm y}(q) := \tfrac{1}{J_{\mathrm y}}\,\gamma_h\big(h\,\xi(p,R,\eta)\big)\,Z_{\mathrm y}(q) \tag{28}$$

for every $q = (p,R) \in Q$, where we suppress the dependence on the parameter h and the filter state η in the notation. The vector field $Z_{\mathrm t}$ describes the direction of the translation motion due to the nonholonomic velocity constraints. The vector field Y_0 will play the role of a drift, which originates from the constant forward force in (21c) and the feedback term $-\lambda\,\sin(\alpha(R))$ in (21d). The configuration-dependent parts of the oscillatory terms in (21d) and (21e) are described by the vector fields $Y_{\mathrm p}$ and $Y_{\mathrm y}$, respectively. Let TQ denote the tangent bundle of Q. The vector fields $Z_{\mathrm t}$, $Z_{\mathrm p}$, $Z_{\mathrm y}$ generate a subbundle $\mathcal{D}$ of TQ. To describe the linear velocity-dependent damping terms in (21c)–(21e), we choose a smooth bundle map $B\colon TQ \to TQ$ such that $B \circ Z_{\mathrm t} = \frac{k}{m} Z_{\mathrm t}$, $B \circ Z_{\mathrm p} = \frac{\kappa_{\mathrm p}}{J_{\mathrm p}} Z_{\mathrm p}$, and $B \circ Z_{\mathrm y} = \frac{\kappa_{\mathrm y}}{J_{\mathrm y}} Z_{\mathrm y}$. Finally, to describe the second-order dynamics of the VYPa, we choose an affine connection ∇ on Q such that $\nabla_Z Z_{\mathrm t} = 0$, $\nabla_Z Z_{\mathrm p} = 0$, and $\nabla_Z Z_{\mathrm y} = 0$ for every vector field Z on Q. Then we can write (21a)–(21e) equivalently as the affine connection system

$$\nabla_{\dot q}\dot q = Y_0(q) - B(\dot q) + \sum_{i=\mathrm{p},\mathrm{y}} \omega\,u^i(\omega t)\,Y_i(q) \tag{29}$$

on Q with velocity constraint $\mathcal{D}$.

We consider the vector fields $Y_{\mathrm p}$ and $Y_{\mathrm y}$ in (29) as control vector fields and the functions $t \mapsto \omega\,u^{\mathrm p}(\omega t)$ and $t \mapsto \omega\,u^{\mathrm y}(\omega t)$ as oscillatory inputs. This point of view allows us to identify system (29) as a member of a certain class of affine connection systems subject to the oscillatory controls. A general averaging theory for this class of systems is established in [17]. It is shown in [17] that, for sufficiently large $\omega > 0$, an oscillatory system of the form (29) approximates the behavior of a certain averaged system. The averaged system involves so-called symmetric products of the control vector fields from the oscillatory system. The averaging analysis in [17] reveals that the symmetric products originate from certain iterated Lie brackets on the tangent bundle of the configuration manifold. Equivalently, without using Lie brackets, the *symmetric product* of two smooth vector fields X and Y on Q can be defined as the vector field

$$\langle X : Y\rangle := \nabla_X Y + \nabla_Y X \tag{30}$$

on Q; see also [35,36]. Recall that the zero-mean anti-derivatives $U^{\mathrm p}$ and $U^{\mathrm y}$ of $u^{\mathrm p}$ and $u^{\mathrm y}$ are assumed to satisfy the orthonormality condition (17). In the terminology of Definition 2, we conclude from the averaging analysis in [17] that the solutions of (29) in the variables

$$\tilde{\dot q} \;=\; \dot q - \sum_{i=\mathrm{p},\mathrm{y}} U^i(\omega t)\, Y_i(q) \tag{31}$$

approximate the solutions of

$$\nabla_{\bar{\dot q}}\bar{\dot q} \;=\; Y_0(\bar q) - B(\bar{\dot q}) - \sum_{i,j=\mathrm{p},\mathrm{y}} \Lambda_{ij}\langle Y_i : Y_j\rangle(\bar q), \tag{32}$$

where the scalar coefficients Λ_{ij} are given by

$$\Lambda_{ij} \;:=\; \frac{1}{2T}\int_0^T U^i(\sigma)\, U^j(\sigma)\,\mathrm{d}\sigma \;=\; \begin{cases} \frac14 & \text{if } i=j, \\ 0 & \text{if } i\neq j. \end{cases} \tag{33}$$

A direct computation shows that the terms with non-vanishing coefficients are given by

$$-\Lambda_{\mathrm{pp}}\,\langle Y_\mathrm{p} : Y_\mathrm{p}\rangle(\bar q) \;=\; \big(\tfrac{\tau_\mathrm{p}}{J_\mathrm{p}} + \tfrac{\lambda}{J_\mathrm{p}}\,\sin(\alpha(\bar R))\big)\, Z_\mathrm{p}(\bar q), \tag{34a}$$

$$-\Lambda_{\mathrm{yy}}\,\langle Y_\mathrm{y} : Y_\mathrm{y}\rangle(\bar q) \;=\; \tfrac{\tau_\mathrm{y}}{J_\mathrm{y}}\, Z_\mathrm{y}(\bar q) \tag{34b}$$

with τ_p and τ_y as in (20). Moreover, one can show that the averaged filter system is the same as the original system (19). In summary, we obtain that the solutions of the closed-loop system (21) in the variables

$$\tilde p \;=\; p, \quad \tilde R \;=\; R, \quad \tilde v \;=\; v, \quad \tilde\eta \;=\; \eta, \tag{35a}$$

$$\tilde\Omega^\mathrm{p} \;=\; \Omega^\mathrm{p} - \frac{1}{J_\mathrm{p}}\, U^\mathrm{p}(\omega t)\,\beta\big(\xi(p,R,\eta)\big), \tag{35b}$$

$$\tilde\Omega^\mathrm{y} \;=\; \Omega^\mathrm{y} - \frac{1}{J_\mathrm{y}}\, U^\mathrm{y}(\omega t)\,\gamma_h\big(h\,\xi(p,R,\eta)\big) \tag{35c}$$

approximate the solutions of

$$\dot{\bar p} \;=\; \bar v\,\bar R e_1, \tag{36a}$$

$$\dot{\bar R} \;=\; \bar\Omega^\mathrm{p}\, X_\mathrm{p}(\bar R) + \bar\Omega^\mathrm{y}\, X_\mathrm{y}(\bar R), \tag{36b}$$

$$m\,\dot{\bar v} \;=\; a - k\,\bar v, \tag{36c}$$

$$J_\mathrm{p}\,\dot{\bar\Omega}^\mathrm{p} \;=\; -\kappa_\mathrm{p}\,\bar\Omega^\mathrm{p} - \lambda\,\sin(\alpha(\bar R)) \tag{36d}$$

$$\qquad - \tfrac12\,\tfrac{\rho}{J_\mathrm{p}}\,(\beta\beta')(\xi(\bar p,\bar R,\bar\eta)) \tag{36e}$$

$$\qquad \cdot \langle \operatorname{grad}\psi(\bar p + \rho\,\bar R e_1), \bar R e_3\rangle, \tag{36f}$$

$$J_\mathrm{y}\,\dot{\bar\Omega}^\mathrm{y} \;=\; -\kappa_\mathrm{y}\,\bar\Omega^\mathrm{y} \tag{36g}$$

$$\qquad - \tfrac12\,\tfrac{\rho}{J_\mathrm{y}}\, h\,(\gamma_h\gamma_h')(h\,(\xi(\bar p,\bar R,\bar\eta)))\,\cos(\alpha(\bar R)) \tag{36h}$$

$$\qquad \cdot \langle \operatorname{grad}\psi(\bar p + \rho\,\bar R e_1), \bar R e_2\rangle, \tag{36i}$$

$$\dot{\bar\eta} \;=\; h\,\xi(\bar p,\bar R,\bar\eta). \tag{36j}$$

In particular, this justifies our statement in the previous section that, for sufficiently large $\omega > 0$, the inputs in (18) have approximately the same effect on (15) as the inputs in (20).

6. Local stability analysis for a radially symmetric signal

As indicated in Section 4, one can expect that, under suitable assumptions, the inputs in (18) lead to a motion of the VYPa along a certain level set of the signal function. A proof of asymptotic stability is, in general, difficult; in particular if the level sets have a complicated shape. In the subsequent analysis, we only investigate the case of spherical level sets. That is, we assume that the signal function ψ is radially symmetric in the following sense.

Assumption 1. There exists a point p_* of $\mathbb{R}^3$ and there exists a smooth real-valued function φ on the half-open interval from 0 to $+\infty$ such that

$$\psi(p) \;=\; \varphi\big(|p-p_*|^2\big) \tag{37}$$

for every $p\in\mathbb{R}^3$, where $|\cdot|$ denotes the Euclidean norm.

From now on, we suppose that Assumption 1 is satisfied with p_* and φ as therein. If φ attains its minimum value at 0, then p_* is the source of the signal. We do not assume that p_* and φ are known; only the existence of p_* and φ must be ensured. Later, we will also impose a certain growth condition on φ to prove asymptotic stability. The assumption that the signal function is radially symmetric is also made in [8] for a kinematic source-seeking VYPa. In [8], it is assumed that the function φ is of the form $\varphi(\sigma) = \psi_* + \mu\,\sigma$ with unknown $\psi_*\in\mathbb{R}$ and $\mu > 0$.

Note that, for every orientation $R\in O$ of the vehicle, the vectors $-Re_2$, $e_3\times(-Re_2)$, e_3 form a positively oriented orthonormal basis for $\mathbb{R}^3$, where $\times$ is the usual cross product. Instead of using the original configuration variables $(p,R)\in Q$, it turns out to be advantageous to carry out the stability analysis in the variables

$$r \;=\; \langle p-p_*, -Re_2\rangle, \tag{38a}$$

$$s \;=\; \langle p-p_*, e_3\times(-Re_2)\rangle, \tag{38b}$$

$$z \;=\; \langle p-p_*, e_3\rangle, \tag{38c}$$

$$\alpha \;=\; \alpha(R), \tag{38d}$$

where $\langle\cdot,\cdot\rangle$ is the Euclidean inner product on $\mathbb{R}^3$. The variables r,s,z are the components of the vector $p-p_*$ relative to the basis $-Re_2$, $e_3\times(-Re_2)$, e_3, and α is the pitch angle defined in (6). Since we assume that the sensed signal is radially symmetric, the four variables in (38) provide a full description of the configuration of the source-seeking VYPa. The squared distance of the sensor to the source can be written as

$$|p+\rho\,Re_1 - p_*|^2 \;=\; d(r,s,z,\alpha), \tag{39}$$

where

$$d(r,s,z,\alpha) \;:=\; r^2 + (s+\rho\,\cos\alpha)^2 + (z+\rho\,\sin\alpha)^2. \tag{40}$$

Recall that the difference $y-\eta$ in (18) and (19) is described by the function ξ defined in (22). By a slight abuse of notation, we use the letter ξ again to describe the difference $y-\eta$ in the variables (38); i.e., we set

$$\xi(r,s,z,\alpha,\eta) \;:=\; \varphi\big(d(r,s,z,\alpha)\big) - \eta. \tag{41}$$

A direct computation leads to the result that the closed-loop system (21) can be equivalently written in the variables (38) as the system

$$\dot r \;=\; s\,\Omega^\mathrm{y}, \tag{42a}$$

$$\dot s \;=\; v\,\cos\alpha - r\,\Omega^\mathrm{y}, \tag{42b}$$

$$\dot z \;=\; v\,\sin\alpha, \tag{42c}$$

$$\dot\alpha \;=\; \Omega^\mathrm{p}, \tag{42d}$$

$$m\,\dot v \;=\; a - k\,v, \tag{42e}$$

$$J_\mathrm{p}\,\dot\Omega^\mathrm{p} \;=\; -\kappa_\mathrm{p}\,\Omega^\mathrm{p} - \lambda\,\sin\alpha + \omega\, u^\mathrm{p}(\omega t)\,\beta\big(\xi(r,s,z,\alpha,\eta)\big), \tag{42f}$$

$$J_\mathrm{y}\,\dot\Omega^\mathrm{y} \;=\; -\kappa_\mathrm{y}\,\Omega^\mathrm{y} + \omega\, u^\mathrm{y}(\omega t)\,\gamma_h\big(h\,\xi(r,s,z,\alpha,R,\eta)\big), \tag{42g}$$

$$\dot\eta \;=\; h\,\xi(r,s,z,\alpha,\eta) \tag{42h}$$

on the open subset $U := \mathbb{R}^3\times(-\pi/2,\pi/2)\times\mathbb{R}^4$ of $\mathbb{R}^8$. Moreover, the change of variables (35) becomes

$$\tilde r \;=\; r, \qquad \tilde s \;=\; s, \qquad \tilde z \;=\; z, \tag{43a}$$

$$\tilde\alpha \;=\; \alpha, \qquad \tilde v \;=\; v, \qquad \tilde\eta \;=\; \eta, \tag{43b}$$

$$\tilde\Omega^\mathrm{p} \;=\; \Omega^\mathrm{p} - \frac{1}{J_\mathrm{p}}\, U^\mathrm{p}(\omega t)\,\beta\big(\xi(r,s,z,\alpha,\eta)\big), \tag{43c}$$

$$\tilde\Omega^\mathrm{y} \;=\; \Omega^\mathrm{y} - \frac{1}{J_\mathrm{y}}\, U^\mathrm{y}(\omega t)\,\gamma_h\big(h\,\xi(r,s,z,\alpha,\eta)\big) \tag{43d}$$

and the averaged system (36) can be written as the system

$$\dot{\bar r} \;=\; \bar s\,\bar\Omega^\mathrm{y}, \tag{44a}$$

$$\dot{\bar{s}} = \bar{v}\cos\bar{\alpha} - \bar{r}\,\bar{\Omega}^{\mathrm{y}}, \quad (44b)$$
$$\dot{\bar{z}} = \bar{v}\sin\bar{\alpha}, \quad (44c)$$
$$\dot{\bar{\alpha}} = \bar{\Omega}^{\mathrm{p}}, \quad (44d)$$
$$m\,\dot{\bar{v}} = a - k\,\bar{v}, \quad (44e)$$
$$J_{\mathrm{p}}\,\dot{\bar{\Omega}}^{\mathrm{p}} = -\kappa_{\mathrm{p}}\,\bar{\Omega}^{\mathrm{p}} - \lambda\sin\bar{\alpha}, \quad (44f)$$
$$-\frac{\rho}{J_{\mathrm{p}}}(\beta\beta')\big(\xi(\bar{r},\bar{s},\bar{z},\bar{\alpha},\bar{\eta})\big) \quad (44g)$$
$$\cdot\,\varphi'\big(d(\bar{r},\bar{s},\bar{r},\bar{\alpha})\big)\,(\bar{z}\cos\bar{\alpha} - \bar{s}\sin\bar{\alpha}) \quad (44h)$$
$$J_{\mathrm{y}}\,\dot{\bar{\Omega}}^{\mathrm{y}} = -\kappa_{\mathrm{y}}\,\bar{\Omega}^{\mathrm{y}} \quad (44i)$$
$$+\frac{\rho}{J_{\mathrm{y}}}\,h\,(\gamma_h\gamma_h')\big(h\,\xi(\bar{r},\bar{s},\bar{z},\bar{\alpha},\bar{\eta})\big) \quad (44j)$$
$$\cdot\,\varphi'\big(d(\bar{r},\bar{s},\bar{r},\bar{\alpha})\big)\,\bar{r}\cos\bar{\alpha} \quad (44k)$$
$$\dot{\bar{\eta}} = h\,\xi(\bar{r},\bar{s},\bar{z},\bar{\alpha},\bar{\eta}) \quad (44l)$$

on U. We already know from Section 5 that the solutions of (21) in the variables (35) approximate the solutions of (36). It follows that the solutions of (42) in the variables (43) approximate the solutions of (44). Thus, as a consequence of Proposition 1, we can state the following implication.

Proposition 2. *If a point x_* of U is locally asymptotically stable for (44), then x_* is practically locally uniformly asymptotically stable for (42) in the variables (43).*

Because of Proposition 2, practical stability for the closed-loop system follows if we can prove local asymptotic stability for the averaged system. A necessary condition for local asymptotic stability is the existence of an equilibrium point. We write such an equilibrium $x_* \in U$ component-wise as

$$x_* = (r_*, s_*, z_*, \alpha_*, v_*, \Omega_*^{\mathrm{y}}, \Omega_*^{\mathrm{p}}, \eta_*). \quad (45)$$

Using that the constants a and k in (44e) are positive, one can easily check that a point $x_* \in U$ is an equilibrium of (44) if and only if the following condition is satisfied:

Assumption 2. The components of x_* in (45) satisfy the equations

$$s_* = 0, \quad z_* = 0, \quad \alpha_* = 0, \quad (46a)$$
$$a = k\,v_*, \quad v_* = r_*\,\Omega_*^{\mathrm{y}}, \quad \Omega_*^{\mathrm{p}} = 0, \quad (46b)$$
$$J_{\mathrm{y}}\,\kappa_{\mathrm{y}}\,\Omega_*^{\mathrm{y}} = \rho\,h\,(\gamma_h\gamma_h')(0)\,r_*\,\varphi'(r_*^2+\rho^2), \quad (46c)$$
$$\eta_* = \varphi(r_*^2+\rho^2). \quad (46d)$$

Suppose that $x_* \in U$ is an equilibrium of (44); i.e., Assumption 2 is satisfied. Then $z_* = 0$ means that the third position component p^3 of the vehicle is equal to the desired value p_*^3. Moreover, the pitch angle α_* and the pitch velocity Ω_*^{p} are both equal to zero. Because of $s_* = 0$ and $a = k\,v_*$, we conclude that the vehicle moves with positive forward velocity v_* in the $(p^3 = p_*^3)$-plane along the circle of radius $|r_*| > 0$ centered at p_*. If r_* is positive, then also Ω_*^{y} is positive, which means that the vehicle moves counter-clockwise around p_*. Otherwise r_* and Ω_*^{y} are negative and the motion around p_* is clockwise. Finally, it follows from (46b) and (46c) that the squared equilibrium radius satisfies the equation

$$\tfrac{J_{\mathrm{y}}\,\kappa_{\mathrm{y}}\,a}{k\,\rho} = h\,(\gamma_h\gamma_h')(0)\,r_*^2\,\varphi'(r_*^2+\rho^2). \quad (47)$$

Note that the expression on the left-hand side of (47) is a positive constant while the expression on the right-hand side of (47) depends on the choice of the parameter $h > 0$ and the design function γ_h.

Next, we derive sufficient conditions to guarantee local asymptotic stability for the averaged system (44). For this purpose, we assume that $x_* \in U$ is an equilibrium of (44) and we compute the linearization of (44) about x_*. Using (46a) and (46d), we compute the Jacobian

$$\begin{bmatrix} 0 & \nu_{rs} & 0 & 0 & 0 & 0 & 0 & 0 \\ \nu_{sr} & 0 & 0 & 0 & \nu_{sv} & 0 & \nu_{\mathrm{sy}} & 0 \\ 0 & 0 & 0 & \nu_{z\alpha} & 0 & 0 & 0 & 0 \\ 0 & 0 & 0 & 0 & 0 & \nu_{\alpha\mathrm{p}} & 0 & 0 \\ 0 & 0 & 0 & 0 & \nu_{vv} & 0 & 0 & 0 \\ 0 & 0 & \nu_{\mathrm{p}z} & \nu_{\mathrm{p}\alpha} & 0 & \nu_{\mathrm{pp}} & 0 & 0 \\ \nu_{\mathrm{y}r} & \nu_{\mathrm{y}s} & 0 & 0 & 0 & 0 & \nu_{\mathrm{yy}} & \nu_{\mathrm{y}\eta} \\ \nu_{\eta r} & \nu_{\eta s} & 0 & 0 & 0 & 0 & 0 & \nu_{\eta\eta} \end{bmatrix} \quad (48)$$

with entries

$$\nu_{rs} := \Omega_*^{\mathrm{y}}, \quad \nu_{sr} := -\Omega_*^{\mathrm{y}}, \quad (49a)$$
$$\nu_{sv} := 1, \quad \nu_{\mathrm{sy}} := -r_*, \quad \nu_{z\alpha} := v_*, \quad (49b)$$
$$\nu_{\alpha\mathrm{p}} := 1, \quad \nu_{vv} := -k/m, \quad (49c)$$
$$\nu_{\mathrm{p}z} := -\tfrac{\rho}{J_{\mathrm{p}}^2}(\beta\beta)'(0)\,\varphi'(r_*^2+\rho^2), \quad (49d)$$
$$\nu_{\mathrm{p}\alpha} := -\lambda/J_{\mathrm{p}}, \quad \nu_{\mathrm{pp}} := -\kappa_{\mathrm{p}}/J_{\mathrm{p}}, \quad (49e)$$
$$\nu_{\mathrm{y}r} := 2\,\tfrac{\rho}{J_{\mathrm{y}}^2}\,h^2\,(\gamma_h\gamma_h')'(0)\,r_*^2\,\varphi'(r_*^2+\rho^2)^2 \quad (49f)$$
$$+\,\tfrac{\rho}{J_{\mathrm{y}}^2}\,h\,(\gamma_h\gamma_h')(0)\,\big(\varphi'(r_*^2+\rho^2) + 2\,r_*^2\,\varphi''(r_*^2+\rho^2)\big), \quad (49g)$$
$$\nu_{\mathrm{y}s} := 2\,\tfrac{\rho}{J_{\mathrm{y}}^2}\,h^2\,(\gamma_h\gamma_h')'(0)\,\rho\,r_*\,\varphi'(r_*^2+\rho^2)^2 \quad (49h)$$
$$+\,2\,\tfrac{\rho}{J_{\mathrm{y}}^2}\,h\,(\gamma_h\gamma_h')(0)\,\rho\,r_*\,\varphi''(r_*^2+\rho^2), \quad (49i)$$
$$\nu_{\mathrm{yy}} := -\tfrac{\kappa_{\mathrm{y}}}{J_{\mathrm{y}}}, \quad (49j)$$
$$\nu_{\mathrm{y}\eta} := -\tfrac{\rho}{J_{\mathrm{y}}^2}\,h^2\,(\gamma_h\gamma_h')'(0)\,r_*\,\varphi'(r_*^2+\rho^2), \quad (49k)$$
$$\nu_{\eta r} := 2\,h\,r_*\,\varphi'(r_*^2+\rho^2), \quad (49l)$$
$$\nu_{\eta s} := 2\,h\,\rho\,\varphi'(r_*^2+\rho^2), \quad \nu_{\eta\eta} := -h. \quad (49m)$$

The characteristic polynomial $\chi : \mathbb{C} \to \mathbb{C}$ of (48) is of the form

$$\chi(\zeta) = (\zeta - \nu_{vv})\,\chi_{\mathrm{p}}(\zeta)\,\chi_{\mathrm{y}}(\zeta), \quad (50)$$

where χ_{p} and χ_{y} are polynomials of degree 3 and 4, respectively. The first factor on the right-hand side of (50) has the negative root ν_{vv}. The second factor is given by

$$\chi_{\mathrm{p}}(\zeta) = \zeta^3 - \nu_{\mathrm{pp}}\,\zeta^2 - \nu_{\mathrm{p}\alpha}\,\nu_{\alpha\mathrm{p}}\,\zeta - \nu_{\mathrm{p}z}\,\nu_{z\alpha}\,\nu_{\alpha\mathrm{p}}. \quad (51)$$

One can check that χ_{p} satisfies the Routh–Hurwitz criterion if and only if the following assumption holds.

Assumption 3. The inequalities

$$\tfrac{k\,\kappa_{\mathrm{p}}\,\lambda}{a\,\rho} > (\beta\beta')(0)\,\varphi'(r_*^2+\rho^2) > 0 \quad (52)$$

are satisfied.

Also the third polynomial χ_{y} in (50) can be computed explicitly. In particular, one can check that

$$2\,\tfrac{a\,h\,\rho}{J_{\mathrm{y}}^2\,k}\,h\,(\gamma_h\gamma_h')(0)\,\tfrac{\partial}{\partial\sigma}\Big|_{\sigma=r_*^2}\sigma\,\varphi'(\sigma+\rho^2) \quad (53)$$

is the constant term of χ_{y}. A necessary condition to ensure that χ_{y} satisfies the Routh–Hurwitz criterion is that (53) is positive. For this reason, we suppose that φ satisfies the following growth condition.

Assumption 4. The inequality

$$\tfrac{\partial}{\partial\sigma}\Big|_{\sigma=r_*^2}\sigma\,\varphi'(\sigma+\rho^2) > 0 \quad (54)$$

is satisfied.

Note that Assumption 4 is always satisfied if φ is of the form $\varphi(\sigma) = \psi_* + \mu\,\sigma$ with $\psi_* \in \mathbb{R}$ and $\mu > 0$ as in [8]. It is left to ensure that the remaining inequalities of the Routh–Hurwitz criterion for χ_y are satisfied. To this end, we demand that the parameter-dependent design function γ_h has the following properties, which can be satisfied by a suitable choice of γ_h.

Assumption 5. There exist positive real numbers $\bar{h}$, b_0, b_1, and b_2 such that

$$h\,(\gamma_h\gamma_h')(0) = b_0 \quad \text{and} \quad b_1 \leq (\gamma_h\gamma_h')'(0) \leq b_2 \tag{55}$$

for every $h \geq \bar{h}$.

Note that the polynomial χ_y depends on the choice of the control parameter $h > 0$. If Assumptions 4 and 5 hold, then one can show that there exists some $h_0 > 0$ such that χ_y satisfies the Routh–Hurwitz criterion for every $h \geq h_0$. The proof of this statement requires lengthy but direct computations and is omitted here.

Recall that the squared equilibrium distance r_*^2 is a solution of Eq. (47). If Assumption 5 is satisfied, then the factor $h\,(\gamma_h\gamma_h')(0)$ in (47) is equal to a constant, and therefore the equilibrium distance $|r_*|$ is independent of the choice of the parameter h.

Suppose that Assumptions 1–5 hold. Then, we may conclude from the findings in the preceding paragraphs that the Jacobian (48) is Hurwitz for sufficiently large $h > 0$. It follows that the averaged system (44) is locally asymptotically stable for sufficiently large $h > 0$. By Proposition 2, this in turn implies that the closed-loop system (42) in the variables (43) is practically locally uniformly asymptotically stable for sufficiently large $h > 0$, where a suitable value of the parameter ω depends on the choice of the parameter h. In summary, we obtain the following stability result for the source-seeking VYPa.

Theorem 1. *Suppose that the unknown scalar signal ψ satisfies Assumption 1. Suppose that x_* is a point of U for which Assumptions 2 and 4 are satisfied. Suppose that the design functions β and γ_h satisfy Assumptions 3 and 5. Then, there exists $h_0 > 0$ such that, for every $h \geq h_0$, the point x_* is practically locally uniformly asymptotically stable for (42) in the variables (43).*

Remark 5. Note that our linearization argument only allows a proof of local asymptotic stability. In particular, we cannot make any statement about the size of the domain of attraction. An investigation of non-local stability properties might be subject of future research.

Remark 6. Recall that the notion of practical local uniform asymptotic stability in Definition 1 demands that the control parameter ω is chosen sufficiently large. If ω is not large enough, then we cannot expect a stable behavior of the closed-loop system. On the other hand, in practical implementations, the range of admissible values of ω is limited by a certain physically reasonable upper bound. If this upper bound is rather small, then the proposed method cannot be successfully applied.

7. Numerical test

We test the proposed source seeking method numerically for the following choice of constants, parameters, and functions. The physical constants m, J_p, J_y, k, κ_p, κ_y are set equal to 1. The constant a that determines the forward force is set equal to 0.1. Also the distance ρ of the sensor to the vehicle center is set equal to 0.1. To simulate the measurements of the unknown scalar signal, we have to select a signal function ψ which satisfies Assumption 1. We choose ψ of the form (37) with source position p_* at the origin and radial function φ defined by $\varphi(\sigma) := -4\,e^{-\sigma/2}$. In the simulations, at each time instance t, we compute the value of ψ at current position of the sensor to obtain the scalar signal value $y(t)$ that is used in the feedback law (18) for the source-seeking vehicle. Next, we specify the components of the feedback law (18). We choose the functions $u^p := \cos$ and $u^y := \sin$ to generate the periodic perturbation signals. Then, the zero-mean anti-derivatives of u^p and u^y satisfy the orthonormality condition (17). The constant λ is set equal to 1. There is a certain degree of freedom in the choice of suitable design functions β and γ_h. Here, we select a function β of the form

$$\beta(x) = \sqrt{2\,\beta_0}\,\sqrt{x + \log(2\,\cosh x)} \tag{56}$$

with some $\beta_0 > 0$. Then, we have $(\beta\beta)'(0) = \beta_0$ (cf. Assumption 3). To satisfy Assumption 5, we choose a design function γ_h of the form

$$\gamma_h(x) = \sqrt{1 + (b_0 + b_1\,h\,x)^2/(b_1\,h^2)} \tag{57}$$

with $b_0, b_1 > 0$. Then, we have $h(\gamma_h'\gamma_h)(0) = b_0$ and $(\gamma_h\gamma_h')'(0) = b_1$ for every $h > 0$. We set $\beta_0 := 15$, $b_0 := 10$, and $b_1 := 40$. For this choice of b_0, we obtain that $r_*^{\pm} = \pm 0.2271$ are two solutions of Eq. (47). Let $x_*^{\pm}$ denote the corresponding equilibria of the averaged system (44), where the remaining components of $x_*^{\pm}$ are given by the equations in Assumption 2. In particular, we get $\Omega_*^{y,\pm} = \pm 0.4404$ for the equilibrium yaw-like velocities. One can also check that Assumptions 3 and 4 are satisfied. We know from the stability analysis in Section 6 that the Jacobian (48) is Hurwitz if the control parameter $h > 0$ is sufficiently large. Here, $h = 10$ turns out to be sufficient. This implies that the points $x_*^{\pm}$ are locally asymptotically stable for the averaged system (44). Because of Proposition 2, it follows that $x_*^{\pm}$ are practically locally uniformly asymptotically stable for (42) in the variables (43).

Fig. 2 shows simulation results for the closed-loop system (21) and for its averaged system (36) in the original variables (p, R) of the state manifold Q. In all simulations, the initial time is 0. The initial velocities are given by the equilibrium velocities of the dynamic VYPa (15) with vanishing inputs; i.e., the initial forward velocity is $v_* = 0.1$ and the initial pitch and angular velocities are zero. The initial position of the vehicle center is the point $(1, 0, 0.3)$ and the filter (19) is initialized by the measured value of the signal at time 0. The initial orientation of the vehicle is described by the vectors $R(0)e_1$, $R(0)e_2$, and $R(0)e_3$ of the body frame; cf. Fig. 1. The left column in Fig. 2 shows results for $R(0)e_1 = +e_2$, $R(0)e_2 = -e_1$, and $R(0)e_3 = e_3$. The right column in Fig. 2 shows results for $R(0)e_1 = -e_2$, $R(0)e_2 = +e_1$, and $R(0)e_3 = e_3$. We can see that, depending on the initial orientation, the vehicle tends either to a counter-clockwise motion (left column) or to a clockwise motion (right column) around the source. For the averaged system, we can observe that the vehicle tends to a motion in the $(p^3 = 0)$-plane along a circle of radius $|r_*^{\pm}| = 0.2271$. The closed-loop system approximates the behavior of the averaged system. We can see in Fig. 2 that the quality of approximation improves with increasing parameter ω.

Declaration of competing interest

The authors declare that they have no known competing financial interests or personal relationships that could have appeared to influence the work reported in this paper.

Data availability

Data will be made available on request

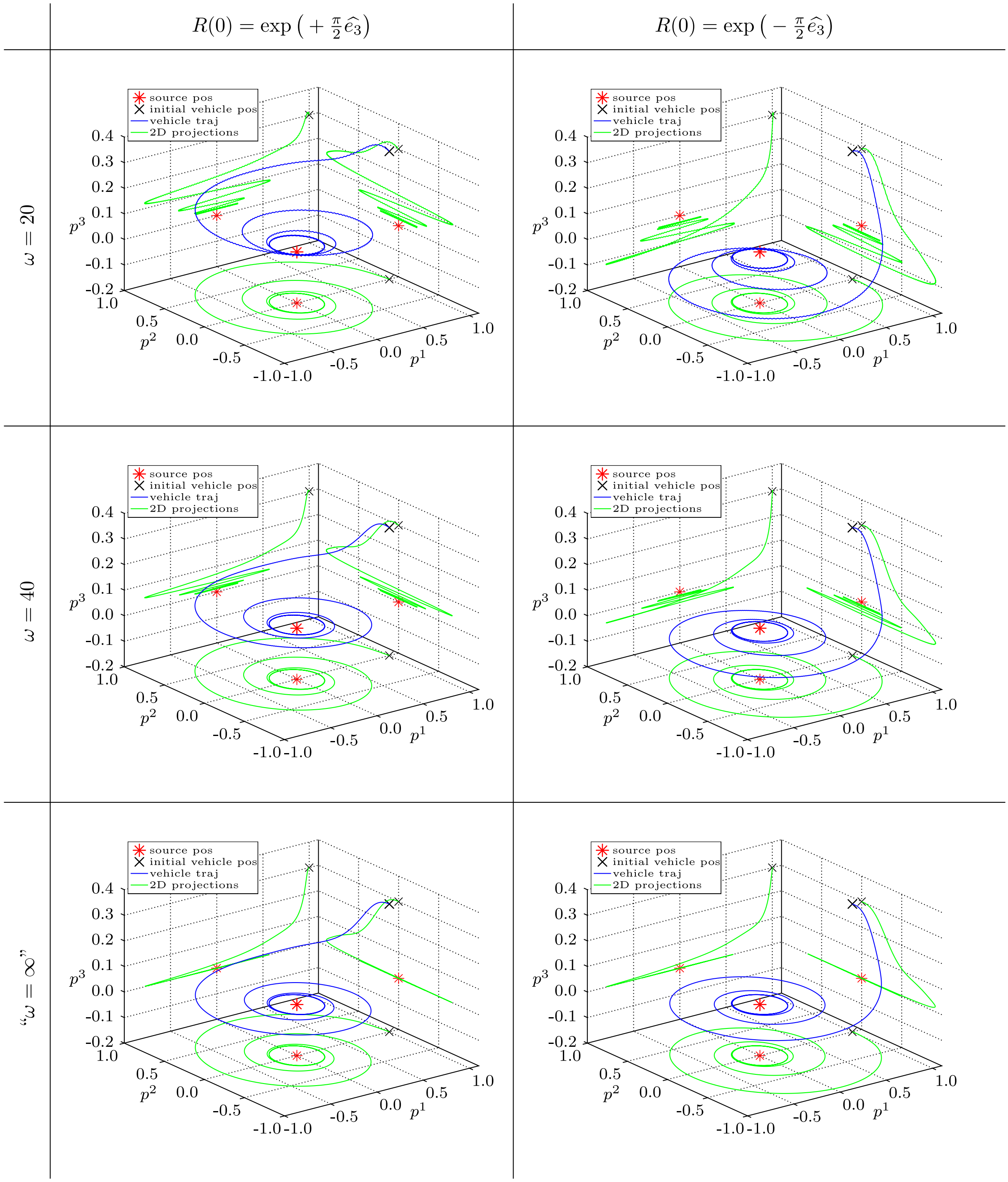

Fig. 2. Simulation results for the initial conditions $p(0) = (1, 0, 0.3)$, $R(0) = \exp(\pm\frac{\pi}{2}\widehat{e_3})$, $v(0) = 0.1$, $\Omega^{y}(0) = 0$, $\Omega^{p}(0) = 0$, $\eta(0) = \psi(p(0) + \rho\, R(0)e_1)$ and different values of the parameter ω. The last row ("$\omega = \infty$") shows the position trajectory of the averaged system. Counter-clockwise motions around the source occur for $R(0) = \exp(+\frac{\pi}{2}\widehat{e_3})$ and clockwise motions occur for $R(0) = \exp(-\frac{\pi}{2}\widehat{e_3})$.

References

[1] C. Zhang, A. Siranosian, M. Krstić, Extremum seeking for moderately unstable systems and for autonomous vehicle target tracking without position measurements, Automatica 43 (10) (2007) 1832–1839.

[2] M.S. Stanković, D.M. Stipanović, Discrete time extremum seeking by autonomous vehicles in a stochastic environment, in: Proceedings of the 48th IEEE Conference on Decision and Control, 2009, pp. 4541–4546.

[3] H.-B. Dürr, M.S. Stanković, K.H. Johansson, A Lie bracket approximation for extremum seeking vehicles, in: Proceedings of the 18th IFAC World Congress, 2011, pp. 11393–11398.

[4] C. Zhang, D. Arnold, N. Ghods, A. Siranosian, M. Krstić, Source seeking with non-holonomic unicycle without position measurement and with tuning of forward velocity, Systems Control Lett. 56 (3) (2007) 245–252.

[5] J. Cochran, M. Krstić, Nonholonomic source seeking with tuning of angular velocity, IEEE Trans. Automat. Control 54 (4) (2009) 717–731.

[6] S.-J. Liu, M. Krstić, Stochastic source seeking for nonholonomic unicycle, Automatica 46 (9) (2010) 1443–1453.

[7] H.-B. Dürr, M. Krstić, A. Scheinker, C. Ebenbauer, Extremum seeking for dynamic maps using Lie brackets and singular perturbations, Automatica 83 (2017) 91–99.

[8] J. Cochran, A. Siranosian, N. Ghods, M. Krstić, 3D source seeking for underactuated vehicles without position measurement, IEEE Trans. Robot. 25 (1) (2009) 117–129.

[9] M.A. Ghadiri-Modarres, M. Mojiri, H.R.Z. Zangeneh, Nonholonomic source localization in 3-D environments without position measurement, IEEE Trans. Automat. Control 61 (11) (2016) 3563–3567.
[10] J. Lin, S. Song, K. You, M. Krstić, Overshoot-free nonholonomic source seeking in 3-D, Internat. J. Adapt. Control Signal Process. 31 (9) (2017) 1285–1295.
[11] A.S. Matveev, M.C. Hoy, A.V. Savkin, 3D environmental extremum seeking navigation of a nonholonomic mobile robot, Automatica 50 (7) (2014) 1802–1815.
[12] R. Fabbiano, C.C. de Wit, F. Garin, Source localization by gradient estimation based on Poisson integral, Automatica 50 (6) (2014) 1715–1724.
[13] M. Abdelgalil, H. Taha, Recursive averaging with application to bio-inspired 3-D source seeking, IEEE Control Syst. Lett. 6 (2022) 2816–2821.
[14] J. Lin, S. Song, K. You, C. Wu, 3-D velocity regulation for nonholonomic source seeking without position measurement, IEEE Trans. Control Syst. Technol. 24 (2) (2016) 711–718.
[15] M. Abdelgalil, H. Taha, Recursive Averaging With Application to Bio-Inspired 3-D Source Seeking, IEEE Control Systems Letters 6 (2022) 2816–2821.
[16] R. Suttner, M. Krstić, Source seeking with a torque-controlled unicycle, IEEE Control Syst. Lett. 7 (2023) 79–84.
[17] F. Bullo, Averaging and vibrational control of mechanical systems, SIAM J. Control Optim. 41 (2) (2002) 542–562.
[18] R. Suttner, Extremum seeking control for an acceleration controlled unicycle, in: Proceedings of the 11th IFAC Symposium on Nonlinear Control Systems, 2019, pp. 676–681.
[19] R. Suttner, M. Krstić, Acceleration-actuated source seeking without position and velocity sensing, in: Proceedings of the 20th IFAC World Congress, 2020, pp. 5348–5355.
[20] B. Wang, S. Nersesov, H. Ashrafiuon, P. Naseradinmousavi, M. Krstić, Underactuated source seeking by surge force tuning: Theory and boat experiments, IEEE Trans. Control Syst. Technol. (2023).
[21] R. Suttner, Z. Sun, Exponential and practical exponential stability of second-order formation control systems, in: Proceedings of the 58th IEEE Conference on Decision and Control, 2019, pp. 3521–3526.
[22] R. Suttner, Extremum seeking control for a class of mechanical systems, IEEE Trans. Automat. Control 68 (2) (2023) 1200–1207.
[23] R. Suttner, M. Krstić, Extremum seeking control for fully actuated mechanical systems on Lie groups in the absence of dissipation, Automatica 152 (2023) 110945.
[24] H.-B. Dürr, M.S. Stanković, C. Ebenbauer, K.H. Johansson, Lie bracket approximation of extremum seeking systems, Automatica 49 (6) (2013) 1538–1552.
[25] A. Scheinker, M. Krstić, Minimum-seeking for CLFs: Universal semiglobally stabilizing feedback under unknown control directions, IEEE Trans. Automat. Control 58 (5) (2013) 1107–1122.
[26] S. Michalowsky, C. Ebenbauer, The multidimensional n-th order heavy ball method and its application to extremum seeking, in: Proceedings of the 53rd IEEE Conference on Decision and Control, 2014, pp. 2660–2666.
[27] M. Krstić, H.-H. Wang, Stability of extremum seeking feedback for general nonlinear dynamic systems, Automatica 36 (4) (2000) 595–601.
[28] Y. Tan, D. Nešić, I. Mareels, On non-local stability properties of extremum seeking control, Automatica 42 (6) (2006) 889–903.
[29] M. Haring, T.A. Johansen, Asymptotic stability of perturbation-based extremum-seeking control for nonlinear plants, IEEE Trans. Automat. Control 62 (5) (2017) 2302–2317.
[30] M. Guay, D. Dochain, M. Perrier, Adaptive extremum seeking control of continuous stirred tank bioreactors with unknown growth kinetics, Automatica 40 (5) (2004) 881–888.
[31] A. Ghaffari, M. Krstić, S. Seshagiri, Power optimization and control in wind energy conversion systems using extremum seeking, IEEE Trans. Control Syst. Technol. 22 (5) (2014) 1684–1695.
[32] P. Paz, T.R. Oliveira, A.V. Pino, A.P. Fontana, Model-free neuromuscular electrical stimulation by stochastic extremum seeking, IEEE Trans. Control Syst. Technol. 28 (1) (2020) 238–253.
[33] L. Moreau, D. Aeyels, Asymptotic methods in stability analysis and control, in: D. Aeyels, F. Lamnabhi-Lagarrigue, A.J. van der Schaft (Eds.), Stability and Stabilization of Nonlinear Systems, in: Lecture Notes in Control and Information Sciences, vol. 246, Springer, London, 1999, pp. 201–213.
[34] F. Bullo, A.D. Lewis, Geometric Control of Mechanical Systems, in: Texts in Applied Mathematics, vol. 49, Springer, New York, 2005.
[35] P.E. Crouch, Geometric structures in systems theory, IEE Proc. D 128 (5) (1981) 242–252.
[36] A.D. Lewis, R.M. Murray, Configuration controllability of simple mechanical control systems, SIAM J. Control Optim. 35 (3) (1997) 766–790.